https://iphopen.org/index.php/se
Online ISSN: 3050-8797 **Print ISSN: 3050-9270**

PREPARATION OF ZNO NPS BY HYDROTHERMAL METHOD AND THE EFFECT OF PREPARATION TEMPERATURE ON NANOSTRUCTURE PROPERTIES

ALI E. HASHIM[1*], RANIA H. HUSSEIN[2], HAMSA M. HAWY[3], MOHAMMED ABDALJABBAR AHMED[4]

[*1,2,3,4]Department of physics, College of Science, University of Dijla, Baghdad, Iraq

***Corresponding Author: Ali E. Hashim**

Abstract

Zinc oxide nanoparticles were prepared by hydrothermal technique under various conditions. The influence of temperature on structure of zinc oxide nanoparticles was studied by x-ray diffraction (XRD) patterns, which confirm the polycrystalline structure of zinc oxide samples. A well-defined diffraction peak at about 36° (101) was observed and this major peak indicates that the hexagonal Structure (ZnO) of zinc oxide was obtained. The field emission-scanning electron microscopy (FE-SEM) studied the surface covered with nanoparticles ,where have different shapes(nanosheets, star shapes and rod), as well as having uniformly distributed over the entire surface and shows that these particles are with average diameter (80.01) ,(60.56) and (152.18)nm respectively. The uv-vis observed small peaks in range (386)nm, absorbance in this region is due to the formation of zinc oxide nanoparticles and the energy band gap was determined in the range 3.1-3.3 eV. The PL spectra showed The recombination of free excitons in the near-band-edge of ZnO caused the peak of the emission locked at around 400 nm in the UV region. FTIR analyses demonstrated Peaks at 564,563 and 750 cm1 are the typical absorption of Zn-O bonds and higher purity of prepared ZnO nano-materials'.

Keywords : *ZnO , Nanoparticles , hydrothermal, XRD, FESEM*

DOI:-10.5281/zenodo.19968240 **Manu script # 453**

Introduction

Transition metal oxide semiconductor nanoparticles have different mechanical, optical, and electrical characteristics. Because of their size and form, these nanostructures may be employed in a variety of areas. [1] Solar cells, light-emitting diodes, gas sensors, and biological probes can all benefit from nanoparticles of various shapes, such as nanorods, nanosheets, and nanobelts. Unit dimensions, form, crystallinity, and lattice constant For a variety of uses [2] Nanoparticles are important in the choosing of these materials. Because the energy problem is expected to be one of the most serious concerns in the near future, research in this area has already begun. , [3,4] optical and electrical properties are exhibited by nanoparticles of ZnO, NiO, TiO2, and other materials, which are crucial for the operation of optoelectronic devices [5] We can offer materials for fabrication units with the aid of structural and optical characterization. The wide bandgap and high exciton binding energy are characteristics of the transition metal oxide semiconductor zinc oxide. Hence Because it belongs to the second and sixth groups of the periodic table, zinc oxide is a semiconductor. It has a direct energy gap which is quite large at (3.37 eV) supplies for electron-gap construction is one of the most preferable materials in optoelectronic research field [6]. It is a low-cost substance that is abundant in nature [7]. ZnO nanoparticles are transparent to visible light while absorbing UV rays. It is a less poisonous, more resistant, and long-lasting substance [8,9]. The morphology of ZnO nanoparticles may be easily modified [10]. Electron mobility in ZnO nanostructures is high [11]. For the synthesis of nanomaterial, many approaches such as chemical vapor deposition, spray pyrolysis, sol-gel method, hydrothermal method, and others are currently available. Techniques for preparation are quite significant in[12,13]. The special advantages of the hydrothermal technique, such as its low cost, minimal preparation needs, and simple equipment, have piqued the interest of various researchers [14].It is a method that is kind to the environment. The hydrothermal process can be used to change the size and shape of nanomaterial. The key determinants of nanoparticle morphology are reaction rate, reaction temperature, and solution concentration. The physical and chemical characteristics of nanoparticles are then impacted by this. Particles are chosen for various uses according to their shape. In this study, we focus primarily on how reaction factors affect the structural and optical characteristics of nanoparticles. Here, the temperature ranges from 100°C to 150°C, and the hydrothermal reaction. Ph of solution mixture is kept as 12 to understand its impact on the development of nanomaterial's [15-17]. Small variations in particle form at the Nano scale have a large influence on their structural and optical characteristics. Reaction parameters can be viewed as tuning factors for the production of nanomaterial that meet our requirements. The influence of temperature on the structural and optical characteristics, as well as the surface nature, was studied in this study over a temperature range not exceeding 150 ° C.

Experimental details:

Sigma-Aldrich zinc chloride ($ZnCl_2$) and ammonia hydroxide (NH_4OH) granules without further purification, all compounds were used of analytical grade. During the experiment, Distilled water was used. The nanoparticles were prepared by using hydrothermal technique. 100 ml of distilled water was used to prepare of 4 g solution of zinc chloride which was stirred for 30 minutes. 25 ml of ammonia-containing NH_4OH solutions were prepared by adding 5 mL of NH_4 to 20 ml of distilled water and stirring for 1 min. Dropping the NH_4OH in the Zinc chloride, and stirring the solution until the pH of the reactants reaches 12. Then the solution was put inside stainless steel container with Thermal-Teflon on its walls, and was firmly closed. This container was put inside oven, for 120 min, and temperature was changed 100, 125, and 150 C. After that, the solution was cooled to room temperature. The result was filtered before being washed with distilled water and placed in a container to dry inside oven.

XRD (6000 SHIMADZ made in japan) was used to measure the average crystallite size and crystal structure. By using an FTIR Model Spectrum TWO Perkin Elmer. (4000 cm1 to 450 cm1), the bonding and purity of the samples were validated. The samples' morphology was examined using FE SEM inspect f 50 fe company. Spectrophotometer Model Lambda 365 Perkin Elme Spectrum range 190-1100 nm double beam was used to measure UV absorption. Spectrophotometer. The Fluoromax spectrofluorometer is used to observe photoluminescence

.

Results and discussion

X-Ray diffraction of ZnO powder

Figure (1a,b,c) shows XRD diffraction patterns of ZnO powder at (100,125 and 150) ^oC with constant time 120 min, which prepared by hydrothermal method. It appears from the X-ray spectrum that the ZnO powder has a polycrystalline structure with 11 peaks in the diffraction spectrum which are (100) ,(002) ,(101), (102), (110), (103), (200) ,(112) ,(112) ,(201) ,(202) this corresponding with the JCPDS data ((JCPDS card No. 79-0207)) which refers to a hexagonal Structure [18-19]. The crystallite size values of ZnO powder were calculated by measuring of half width of the peak maximum intensity (FWHM), and (2θ) of the directions' peaks using Scherer's equation as shown in Table (1a,b,c). The strong and narrow peaks may be ascribed to the preferential

growth along (101) plane of ZnO crystallites. The strain (δ) and dislocation density (η) were calculated and listed in Table (1)

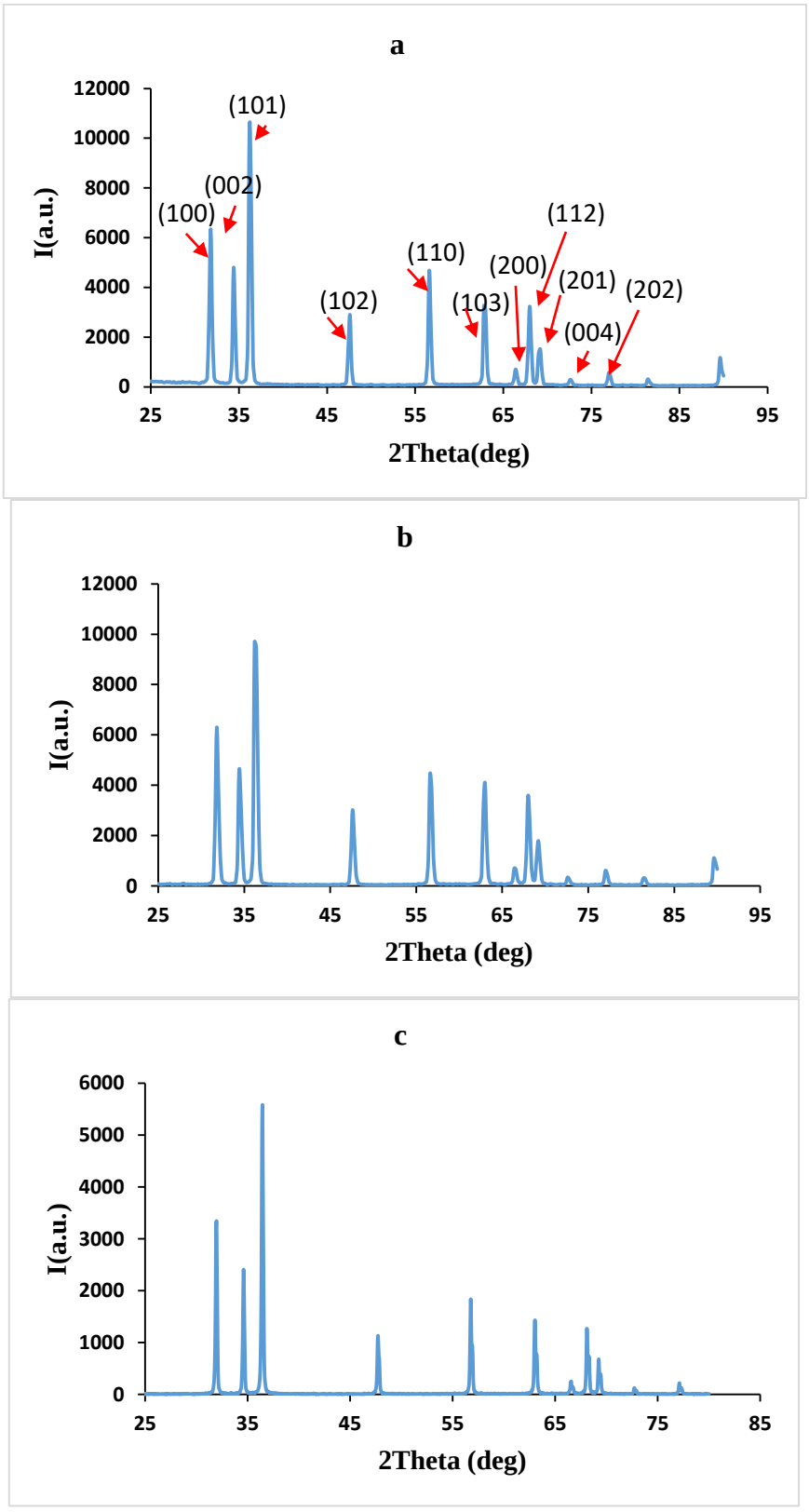

Fig.(1) XRD diffraction of ZnO powder : (a) at 100 ^{o}C, (b) at 125 ^{o}C and (c) at 150 ^{o}C, with constant time 120 min .

Table (1a)) Shows structural parameters crystallite size and FWHM of ZnO nanoparticle.

2 θ (deg)	d observed (Å)	FWHM (deg)	D (nm)	$\delta \times 10^{14}$ lines.m^{-2}	$\eta \times 10^{-4}$ lines^{-2}.m^{-4}
31.8	2.8	0.50	29.24	11.84	11.69
34.4	2.60	0.48	30.46	11.73	10.77
36.2	2.47	0.49	29.24	11.61	11.32
47.6	1.91	0.48	30.46	11.37	10.77
56.6	1.62	0.47	30.10	11.37	10.33
62.8	1.47	0.48	30.46	11.37	10.77
66.4	140	0.47	31.10	11.13	10.33
68.8	1.37	0.49	29.84	11.61	11.23
69.2	1.35	0.52	28.11	12.32	12.64
73.4	1.29	0.50	29.24	11.84	11.69
77.1	1.23	0.49	29.84	11.61	11.23

Table (1b)) Shows structural parameters crystallite size and FWHM of ZnO nanoparticle..

2 θ (deg)	d observed (Å)	FWHM (deg)	D (nm)	$\delta \times 10^{14}$ lines.m^{-2}	$\eta \times 10^{-4}$ lines^{-2}.m^{-4}
31.8	2.81	0.5	29.24	11.84	11.69
34.4	2.60	0.48	30.46	11.37	10.77
36.2	2.47	0.49	29.84	11.61	11.23
47.6	1.91	0.48	30.46	11.37	10.77
56.6	1.62	0.47	31.10	11.13	10.33
63	1.47	0.48	30.46	11.37	10.77
66.4	1.40	0.47	31.10	11.13	10.33
68	1.37	0.49	29.84	11.61	11.23
69.2	1.35	0.52	28.11	12.32	12.64
72.8	1.29	0.5	29.24	11.84	11.69
77	1.23	0.49	29.84	11.61	11.23

Table (1c) Shows structural parameters crystallite size and FWHM of ZnO nanoparticle.

2 θ (deg)	d observed (Å)	FWHM (deg)	D (nm)	$\delta \times 10^{14}$ lines.m^{-2}	$\eta \times 10^{-4}$ lines^{-2}.m^{-4}
31.8	0.18	0.50	81.23	4.26	1.51
34.4	0.17	0.48	86.01	4.02	1.35
36.2	0.18	0.49	81.23	4.26	1.51
47.6	0.18	0.48	81.23	4.26	1.51
56.6	0.17	0.47	86.01	4.02	1.35
63	0.17	0.48	86.01	4.02	1.35
66.4	0.18	0.47	81.23	4.26	1.51
68	0.17	0.49	86.01	4.02	1.35
69.2	0.17	0.52	86.01	4.02	1.35
73	0.17	0.50	86.01	4.02	1.35
77.2	0.17	0.49	86.01	4.02	1.35

Field emission Scanning electron microscope of ZnO

. Figure (2a,b,c) shown FE-SEM images, show that the surface is covered with particles have different shapes(nanosheets, star shapes and rod), which are uniformly distributed over the entire surface and shows that these particles are with average diameter (80.01) ,(60.56) and (152.18)nm respectively, where it note some of particles tend to agglomerates. This result agree with [20,21].

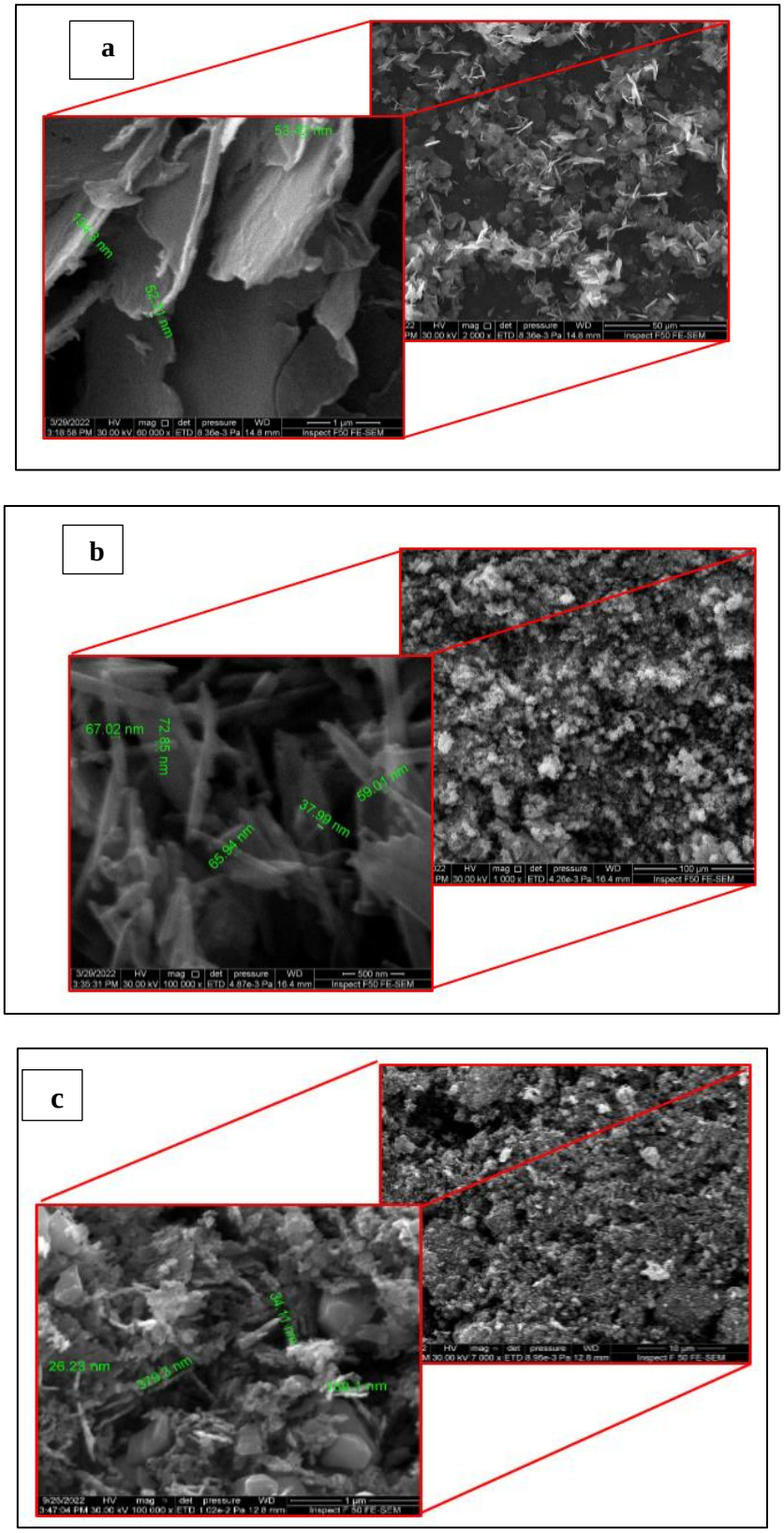

Fig. (2) FE-SEM images of ZnO: (a) at 100C, (b) at 125 C and (c) at 150 C, with constant time 120 min.

Optical properties (UV-Visible spectroscopy)

Figure (3) shows absorbance spectra of ZnO colloidal in range (200-1100), it observed small peaks in range (386)nm, absorbance in this region is due to the formation of zinc oxide nanoparticles [22] . The absorption peak centred at 386 nm is the characteristic peak for hexagonal wurtzite ZnO, this corresponding with XRD results [23].

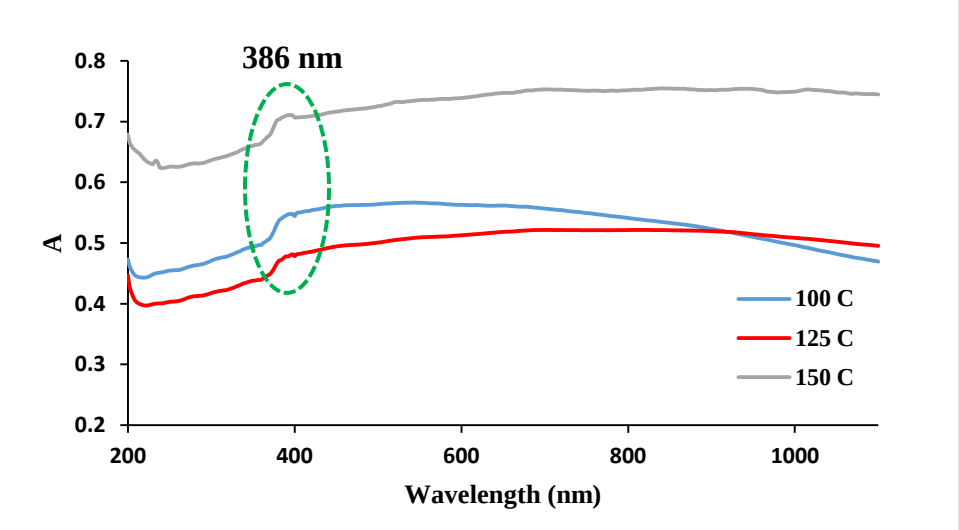

Fig. (3) UV-Visible spectra of ZnO NPs: (a) at 100C, (b) at 125 C and (c) at 150 C, with constant time 120 min.

Through Tauc equation by plotting the relation $(\alpha\ hv)^2$ versus photon energy (hv) and extrapolation the linear portion of the curve to absorption equal to zero as given in Figures (3 a,b,c). The energy gap of ZnO at (100,125 and 150) C with constant time 120 min, which prepared by hydrothermal method was found (3.1,3.2 and 3.3)eV respectively as shown in Figure (3a,b,c). The amount of reflectivity depends on the incident wavelength, the surface roughness, and the angle between the incident beam and the surface of the cell. Figure (4) shows the reflectance of ZnO, as function of wavelength in range (200-1100)nm. It note the values of the reflectance decrease at short wavelengths (<400nm) to record 0.08,0.07 and 0.17 at wavelength 200nm.

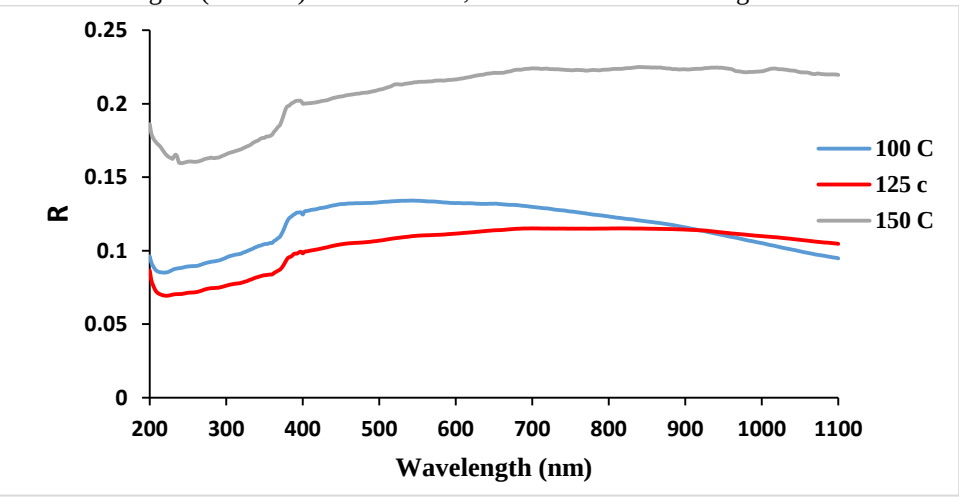

Figure (4) Reflectance spectra of ZnO: (a) at 100C, (b) at 125 C and (c) at 150 C, with constant time 120 min.

The refractive index is an important parameter for semiconductor materials and applications, the refractive index calculated from the relationship ($n = \frac{1+R^{0.5}}{1-R^{0.5}}$) to all samples. The refractive index as a function of the reflectivity (R), depends on several factors, including the type of material and the crystal structure, the refractive index values vary depending on the change of roughness of the samples surface. Figure (5) shows change of refractive index of ZnO a function of wavelength in range (200-1100) nm for all samples, the curves similar to the reflectivity curve of each sample. The Refractive index reaches its maximum value of (2.9, 1.9 and 2.6) at wavelength 400 nm. it note the refractive index change with increase temperature This can be attributed to the changes induced in crystalline size and microstrain of ZnO crystals that leads to change in surface morphology and vacancies inside the crystal structure.

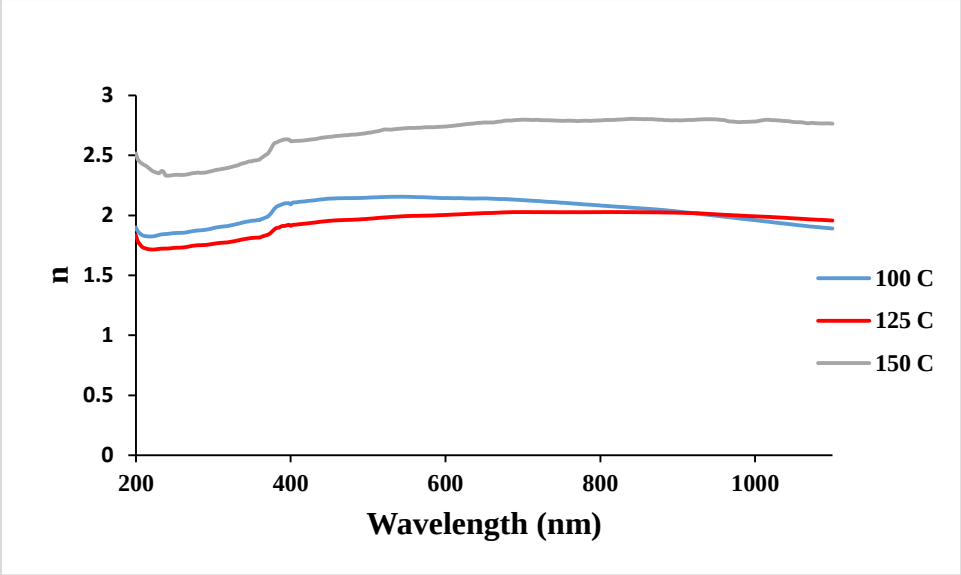

Fig. (5) refractive index of ZnO: (a) at 100C, (b) at 125 C and (c) at 150 C, with constant time 120 min.

The optical characteristics of ZnO NPs generated by hydrothermal technique were investigated using a photoluminescence (PL) research at room temperature. Figure (6) shows PL spectra (6). The PL spectra of ZnO showed two peaks. The recombination of free excitons in the near-band-edge of ZnO caused the peak of the emission locked at around 400 nm in the UV region. The Si substrate was usually ascribed to the other peak, which displayed widespread emission in the IR range. It is worth noting that the peak at 600nm in the sample at 125 C was attributable to oxygen vacancies. [24,25],

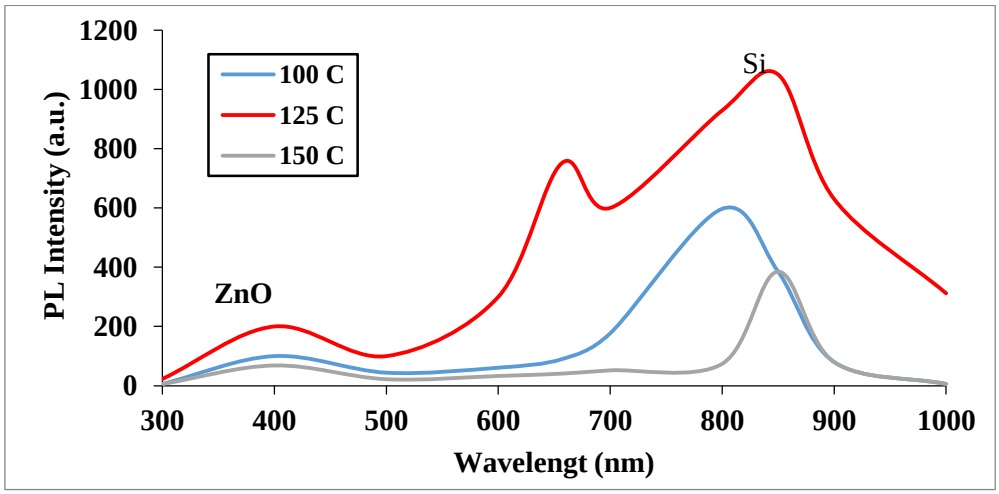

Fig.(6) PL spectrum of ZnO at 100C, 125 C and 150 C, with constant time 120 min.

The FT-IR spectra of ZnO NPs generated by hydrothermal technique with a wavenumber range of 500 to 4500 cm1 is shown in Fig (7a,b,c). take note of Peaks at 564,563 and 750 cm1 are the typical absorption of Zn-O bonds; peak absorption in this range indicates hexagonal phase ZnO, which corresponds with XRD; peak at 3404 cm1 is the absorption of O-H. The range (2926 and 2855 cm-1) is connected to C-H, and the peak at 2359 cm-1 can be attributed to C=C absorption. Peak at 1744 cm-1 can be ascribed to C=O absorption, whereas peaks at 1653, 1456 cm-1, and 1076 cm-1 are connected to C-H and C-N, respectively [26,27].

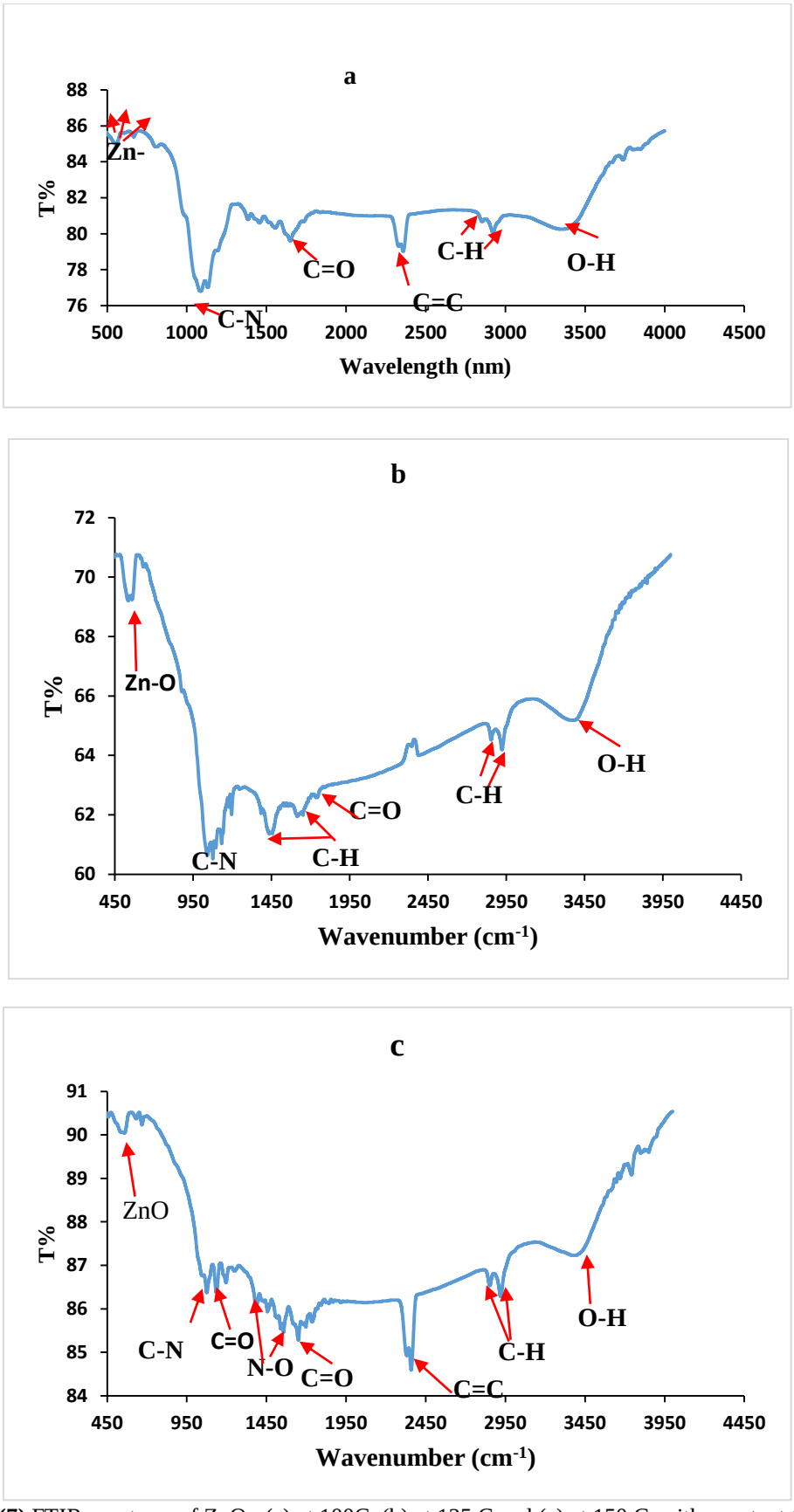

Fig.(7) FTIR spectrum of ZnO : (a) at 100C, (b) at 125 C and (c) at 150 C, with constant time 120 min.

Conclusion

High quality and homogeneity Zinc oxide (ZnO) nanoparticles were successfully prepared using hydrothermal technique. As a preparing condition, temperature plays a key role for controlling the structural characteristics of such oxide. An increase in temperature by no more than 200°C then it starts to decompose can change the nanostructure shapes (nanosheets, star shapes and rod), as well as change average diameter of the nanoparticles. The uv-vis was observed, a increase in energy band gap in the range 3.1-3.3 eV. The PL spectra showed the recombination of free exactions in the near-band-edge o caused the absorbance of incident rays in the longest wavelength range in ultraviolet rays. FTIR analyses demonstrated the typical absorption of Zn-O bonds and higher purity of prepared ZnO nano-materials'.

References

[1] Pan L, Xu B, Tang J and Wang F 2013 Synthesis of sheet-like nanoscaled ZnO and Ag/ZnO composite nanocrystals and theirelectrocatalytic properties Micro Nano Lett. 8 378–82- Habeeb AlshamsiHA and Hussein B S 2018 Hydrothermal preparation of silver doping zinc oxide nanoparticles: studys,
characterization and photocatalytic activities Orient. J. Chem. 34 1898–907

[2] Qiu J, Weng B, Zhao L, Chang C, Shi Z, Li X, Kim H-K and Hwang Y-H 2014 Synthesis and characterization of flower-like bundles of ZnO nanosheets by a surfactant-free hydrothermal process J. Nanomater. 2014 281461

[3] VellakkatMand DevendrappaH2016 Chitosan mediated synthesis of core/double shell/ternary polyaniline/chitosan/cobalt oxidenanocomposite-as high energy storage electrode material in supercapacitors Mater. Res. Express 3 015502 -

[4] HossainMK, Firoz Pervez M, MiaMNH, Mortuza A A, RahamanMS, KarimMR, Islam JMM, Ahmed F and MubarakAK2017Effect of dye extracting solvents and sensitization time on photovoltaic performance of natural dye sensitized solar cells Results inPhysics 7 1516–23Excellent

[5] Ko SH, Lee D, KangHW,NamKH, Yeo J Y, Hong S J, Grigoropoulos CP and SungHJ 2011 Nanoforest of hydrothermally grownhierarchical ZnO nanowires for a high efficiency dye-sensitized solar cell 666–71 -. [9] Wang Z L 2004 Zinc oxide nanostructures: growth, properties and applications J. Phys.: Condense. Matter 16 R829–58

[6]] AyeleruOO, Dlova S, Ntuli F, Kehinde W, KupolatiWKand Olubambi P A 2019 Development and size distribution of polystyrene/ZnO nanofillers Procedia Manufacturing 30 194–9 – [18] Miao Y, Zhang H, Yuan S, Jiao Z and ZhuX2016 Preparation of flower-like ZnO architectures assembled with nanosheets forenhanced photocatalytic activity J. Colloid Interface Sci. 462 9–18

[7]] UI Haq AN, Nadhman A, Ullah I, Mustafa G, YasinzaiMand Khan I 2017 Synthesis approaches of ZnO nanoparticles. The dilemma ofecotoxicity 2017 8510342 .

[8] Karthik K, Dhanuskodi S, Gobinath C, Prabukumar S and Sivaramakrishnan S 2018 Multifunctional properties of microwave assistedCdO–NiO–ZnO mixed metal oxide nanocomposite: enhanced phocatalytic and antibacterial activities J. Mater. Sci., Mater. Electron. 295459–71

[9] Baruah S and Dutta J 2009 Hydrothermal growth of ZnO nanostructures Sci. Technol. Adv. Mater. 10 013001]

[10]] ChuHO, Wang Q, Shi Y-J, Song S-Geng, Liu W-Guo, Zhou S, Gibson D, Alajlani Y and LiC2020 Structural, optical properties andoptical modelling of hydrothermal chemical growth derived ZnO nanowires Trans. Nonferrous Met. Soc. China 30 191–9

[11] Hassanpour M, Safardoust-HojaghanHand Salavati-NiasariM2017 J. Mater. Sci.: Mater. Electron. 28 10830–7

[12] Miao Y, Zhang H, Yuan S, Jiao Z and ZhuX2016 Preparation of flower-like ZnO architectures assembled with nanosheets for
enhanced photocatalytic activity J. Colloid Interface Sci. 462 9–18

[13] Bhawna, Majee B P, Choudhari V, Prakash R and Mishra AK2019 Hydrothermally grown ZnO nanoparticles for photodegradation of textile dye AIP Conf. Proc. 2100]

[14]] Suresh BabuKand NarayananV2013 Hydrothermal synthesis of hydrated zinc oxide nanoparticles and its characterization Chem. Sci.Trans.4336

[15] ChuHO, Wang Q, Shi Y-J, Song S-Geng, Liu W-Guo, Zhou S, Gibson D, Alajlani Y and LiC2020 Structural, optical properties andoptical modelling of hydrothermal chemical growth derived ZnO nanowires Trans. Nonferrous Met. Soc. China 30 191–9

[16] Aneesh PM, Vanaja KA and JayarajMK2007 Synthesis of ZnO Nanoparticles by hydrothermal method Proc. of SPIE 6639

[17] Raji R and Gopchandran KG2017 ZnO nanostructures with tunable visible luminescence; effects of kinetics of chemical reduction andannealing 2 51–8

[18] Pung Swee-Yong, Lee Wen-Pie, Aziz Azizan (2012) Kinetic study of organic dye degradation using ZnO particles with different morphologies as a photocatalyst. Inte J Inorg Chem 2012:1–9

[19]Wali Muhammad, Naimat Ullah, Muhammad Haroon and Bilal Haider Abbasi"Optical, morphological and biological analysis of zinc oxide nanoparticles (ZnO NPs) using *Papaver somniferum* L." : RSC Adv., 2019, Vol. 9, 29541–29548

[20] Chin Boon Onga , Law Yong Ngb , Abdul Wahab Mohammad ,"A review of ZnO nanoparticles as solar photocatalysts: Synthesis, mechanisms and applications", Renewable and Sustainable Energy Reviews 81 (2018) 536–551

[21] Mojtaba Abbasian1,*, Nafiseh Khakpour A.Ali , and Solmaz Esmaeily Shoj," Synthesis of Poly (methyl methacrylate)/Zinc OxideNanocomposite with Core-Shell Morphology by AtomTransfer Radical Polymerization" , Journal of Macromolecular Science, Part A: Pure and Applied Chemistry (2013) 50, 966–975

[22] Vijayakumar, C. Krishnakumar, P. Arulmozhi, S. Mahadevan, N. ParameswariBiosynthesis, characterization and antimicrobial activities of zinc oxide nanoparticles from leaf extract of Glycosmis pentaphylla (Retz.) DC Microb. Pathog., 116 (2018), pp. 44-48

[23] A. J. Wooten, D. J. Werder, D. J. Williams, J. L. Casson, and J. A. Hollingsworth (2009). J Am Chem Soc 131, 16177.

[24] Yang, P.; Yan, H.; Mao, S.; Russo, R.; Johnson, J.; Saykally, R.; Morris, N.; Pham, J.; He, R.; Choi, H.-J. Controlled growth of ZnO nanowires and their optical properties. Adv. Funct. Mater. 2002, 12, 323.

[25] Prabhakar, R.R.; Pramana, S.S.; Karthik, K.R.G.; Sow, C.H.; Jinesh, K.B. Efficient multispectral photodetection using Mn doped ZnO nanowires. J. Mater. Chem. 2012, 22, 13965. [CrossRef]

[26]] Srinivasa Rao, N. and Basaveswara Rao, M.V. (2015) Structural and Optical Investigation of ZnO Nanopowders Synthesized from Zinc Chloride and Zinc Nitrate. American Journal of Materials Science, 5, 66-68.

[27]R. Koole, E. Groeneveld, D. Vanmaekelbergh, A. Meijerink & C. D.M. Doneg, "Size Effects on Semiconductor Nanoparticles", Nanoparticles, workhorses of nanoscience, de Mello Donega (Ed.), Springer, ISBN: 978-662-44822-9, (2014) .